Author(s): Pöykkö, S. & Puska, M. J. & Nieminen, Risto M.

Title: Nitrogen-impurity native-defect complexes in ZnSe

Year: 1998

Version: Final published version

Please cite the original version:

Pöykkö, S. & Puska, M. J. & Nieminen, Risto M. 1998. Nitrogen-impurity native-defect complexes in ZnSe. Physical Review B. Volume 57, Issue 19. 12174-12180. ISSN 1550-235X (electronic). DOI: 10.1103/physrevb.57.12174.

Nitrogen-impurity–native-defect complexes in ZnSe

S. Pöykkö,* M. J. Puska,† and R. M. Nieminen‡
Laboratory of Physics, Helsinki University of Technology, Helsinki FIN-02015 HUT, Finland
(Received 28 August 1997)

Total-energy calculations for defect complexes formed by nitrogen impurities and native defects in ZnSe are reported. Complexes formed by a substitutional nitrogen bound to a zinc interstitial or a selenium vacancy are shown to be the most probable candidates for the compensating defect in *p*-type ZnSe. Our results also show that the clustering of defects in ZnSe is an energetically favored process. This may explain the short lifetimes of ZnSe-based devices. [S0163-1829(98)00519-0]

I. INTRODUCTION

Due to the large direct band gap and the almost perfect lattice match to GaAs, ZnSe is a promising material for many semiconductor applications. It is generally accepted that most of the problems hindering the fabrication of properly doped ZnSe materials and the technological use of ZnSe are related to point defects.[1] It has been extremely difficult to obtain effective *p*-type doping. Acceptor concentrations of the order of the 10^{18} cm^3 have been achieved by using nitrogen rf-plasma sources, but additional nitrogen is fully compensated.[2,3] Moreover, even if the doping problems of ZnSe have been overcome, the lifetimes of electronics components, such as blue-light emitting lasers, are often limited due the rapid generation of defects in the lattice.

A detailed understanding of the compensation mechanism hindering the *p*-type doping is still lacking. Laks and co-workers have shown that the concentrations of various native defects are so low that they cannot cause the doping problem.[4,5] The nitrogen solubility has also been suggested to limit the doping efficiency, but the measured nitrogen concentrations are shown to exceed 10^{19} cm^{-3} whereas the effective acceptor concentration $(N_A - N_D)$ is limited to 10^{18} cm^{-3}.[6] Chadi and co-workers have proposed that large lattice relaxations near the dopant atom may turn the shallow acceptor states to states deep in the band gap.[7–11] Among large lattice relaxation models the double broken bond model[11] is argued to be the most probable one for N-doped ZnSe. The formation of N_2 molecules has also been proposed to cause compensation.[12] Finally, Garcia and Northrup[13] concluded from first-principles calculations for As-doped ZnSe that the formation of dopant-impurity–native-defect pairs is the reason for the saturation of hole concentration.

Following Garcia and Northrup,[13] we have made first-principles calculations for various dopant–native-defect complexes in ZnSe. We use nitrogen as the impurity atom and show that its properties are substantially affected by strong lattice relaxation. This is in contrast with behavior of the other common *p*-type dopant candidates, P and As. Our results for the formation and binding energies of the defect complexes show that their formation at high nitrogen concentrations is the likely reason for the saturation of the doping efficiency.

The organization of the present paper is as follows: In Sec. II we describe the details of our numerical methods. Section III is devoted to the presentation and discussion of the results obtained, and Sec. IV contains our conclusions.

II. METHODS

Our calculations are based on the density-functional theory with the electron exchange-correlation treated in the local-density approximation (LDA).[14] Because the ionic relaxations in ZnSe lattice are generally quite large due to the softness of the material and because the defect complexes studied here include also defect clusters, we have calculated the electronic structures and the lattice relaxations for the lowest formation energy defects in ZnSe using a large supercell of 64-atom sites in order to minimize the defect-defect interactions. The Brillouin-zone sampling consists of the $2\times2\times2$ Chadi-Cohen **k**-point mesh.[15] In our previous study of point defects in GaAs the above supercell size and **k**-point sampling have been shown to give well-converged results.[16] For the Zn and Se ions we use the standard Hamann pseudopotentials.[17] The Zn $3d$-electrons are included in the core, but the nonlinear core-valence corrections[18] are used to account for the overlap of the core and the valence-electron charges. This method has been shown to give reasonably accurate formation energies for defects in ZnSe.[12] For the N ion the Vanderbilt ultrasoft pseudopotential[19] has been employed in order to reduce the number of plane waves needed to describe electron wave functions. As a result of the use of the ultrasoft pseudopotentials already a relatively small cutoff energy of 27 Ry gives well-converged results.[21] According to our calculations for the bulk ZnSe the equilibrium lattice constant is 5.61 Å, which is slightly less than the experimental value of 5.67 Å. This kind of discrepancy is typical for the LDA calculations. The theoretical lattice constant has been used in all our defect calculations.

Our pseudopotential-plane-wave calculations give for simple point defects in ZnSe formation energy values that quite accurately coincide with those obtained by all-electron calculations.[20] All calculations have been performed in a massively parallel CRAY-T3E system using the carefully optimized FINGER (FINnish General Electron Relaxator) code (see the Appendix for details).

In our defect calculations all the ions in the supercell have been allowed to relax without any symmetry constraints in order to attain the minimum-energy configuration. This re-

laxation is performed using the effective Broyden-Fletcher-Goldfarb-Shanno (BFGS) algorithm.[22] The initial atomic configurations have been randomized slightly from the ideal structure to remove any spurious symmetries.

The formation energy $\Omega(D_i)$ of the defect D_i in the charge state Q_i can be written as[13]

$$\Omega(D_i)=E_D+Q_i(\mu_e+E_v)+\lambda\Delta H(n_{\mathrm{Zn}}-n_{\mathrm{Se}}) +(n_{\mathrm{Se}}-n_{\mathrm{Zn}})\mu_{\mathrm{Zn}}^{\mathrm{bulk}}-n_{\mathrm{Se}}\mu_{\mathrm{ZnSe}}-n_{\mathrm{N}}\mu_{\mathrm{N}}, \quad (2.1)$$

where E_D is the total energy of the defect supercell, n_X ($X=\mathrm{Se,Zn,N}$) is the number of ions of the type X in the supercell, and μ_e is the electron chemical potential measured with respect to the valence-band maximum. The chemical potential of the ZnSe pair in ZnSe is μ_{ZnSe}, $\mu_{\mathrm{Zn}}^{\mathrm{bulk}}$ is the chemical potential of a Zn atom in bulk Zn. ΔH is the heat of formation of ZnSe. The parameter λ fixes the stoichiometry; it can vary from 0 to 1 so that $\lambda=0$ gives the formation energy in Zn-rich conditions and $\lambda=1$ in Se-rich conditions. For the chemical potential of the nitrogen atom (μ_{N}) we use the chemical potential of the N atom in the (N_2) dimer. Actually, the absolute value of the chemical potential μ_{N} is difficult to determine exactly. However, in this paper we present results, besides for the native defects, only for complexes containing one impurity atom. Then the formation energy differences between the different impurity-defect complexes are independent of μ_{N}, making the comparison of the corresponding formation energies reliable. This is in contrast, for example, to the case in which one compares the formation energy of the substitutional N_2 dimer defect with that of the substitutional N impurity.

III. RESULTS

A. Native defects

The native defects in ZnSe with the lowest formation energy in *p*-type material grown under zinc-rich conditions are the selenium vacancy (V_{Se}) and the tetrahedral zinc interstitial (Zn_i) surrounded by four nearest-neighbor Se ions.[5,20,13] The thermodynamically stable charge states for V_{Se} are the neutral and the doubly positive one. Since the singly positive charge state is not the stablest charge state for any value of the electron chemical potential, V_{Se} is a so-called negative-effective *U* defect. For Zn_i we are able accurately to calculate only the doubly positive state because of the narrow LDA band gap of 1.1 eV. The highest occupied electron state in the singly positive and neutral charge states turns out to be higher in energy than the band minimum of the LDA conduction band. Therefore when trying to calculate these charge states a delocalized conduction-band state will be occupied instead of the proper localized defect state in the band gap. One can contrast this difficulty with the experiments, according to which Zn_i has an ionization level from 1+ to 2+ at 1.9 eV above the top of the valence-band maximum.[23] The formation energies of the native defects of the different charge states are given in Table I. The ensuing ionization levels (i.e., the positions of the Fermi level at which the charge state of the defect changes) are also given in Table I.

The lattice relaxations around the doubly positive and the neutral selenium vacancies are large (see Fig. 1). The nearest-neighbor Zn ions of the doubly positive vacancy relax symmetrically *outwards* from the defect center. The amplitude of the relaxation is about 24 percent of the perfect-lattice bond length. According to our calculations, the neutral vacancy has an interesting symmetry-breaking, trigonal relaxation mode in which one of the nearest-neighbor Zn ions has relaxed in the [111] direction towards the interstitial tetrahedral site whereas the remaining three nearest-neighbor Zn ions relax symmetrically towards a ''defect center.'' The total energy of the defect in this relaxation mode is about 0.2 eV lower than that corresponding to a totally symmetric breathing relaxation conserving the T_d symmetry. The driving force behind the symmetry breaking cannot be the normal Jahn-Teller effect because in the symmetric configuration the two highest occupied single-electron states are the nondegenerate totally symmetric a_1 states of the T_d point-symmetry group. Before the ionic relaxation, i.e., for the ideal vacancy, the uppermost occupied state is close to the conduction band. The ionic relaxation lowers it so that in both symmetry modes the state is finally a few tenths of an eV below the valence-band maximum.

TABLE I. Native defects in ZnSe with the lowest formation energies. The calculated formation energies [Eq. (2.1)], relaxation energies (E_{rel}), and ionization levels are given. All the energies given are in eV. The calculated value for the heat of formation (ΔH) is 1.5 eV.

Defect	Formation energy	E_{rel}	Ionization levels
$(V_{\mathrm{Se}})^{2+}$	$0.14+\lambda\Delta H+2\mu_e$	1.58	(2+/0) 1.35
$(V_{\mathrm{Se}})^{0}$	$2.55+\lambda\Delta H$	0.49	
$(\mathrm{Zn}_i)^{2+}$	$-1.15+\lambda\Delta H+2\mu_e$	0.60	
$(V_{\mathrm{Zn}})^{2-}$	$4.462-\lambda\Delta H$	0.54	

The relaxation energy (defined as the total-energy difference between the ideal and the fully relaxed structures) is given in Table I for the Se vacancy in the neutral (trigonal-symmetry) and in the doubly positive charge states. The

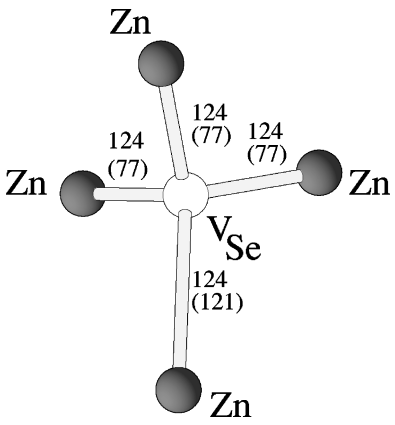

FIG. 1. Ionic structure of the selenium vacancy in ZnSe. The center of the vacancy (white sphere) is defined as the position of a Se atom in a perfect lattice and by assuming that atoms far from the vacancies in the vacancy superlattice do not move from their ideal lattice positions. The distances of the Zn ions (gray spheres) from the vacancy center are given in percent of the bond length in the ideal lattice for the doubly positive (upper numbers) and for the neutral (numbers in parentheses) charge states.

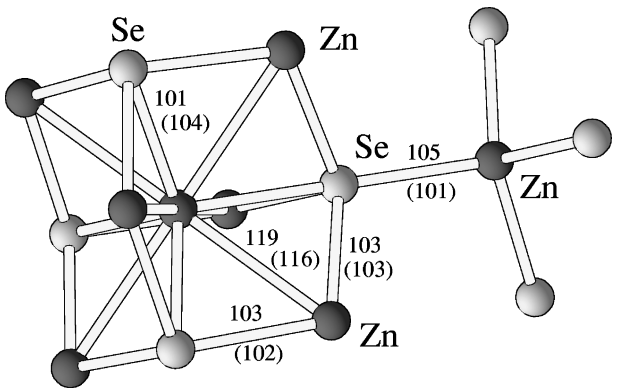

FIG. 2. Ionic structure of the tetrahedral zinc interstitial (dark-gray sphere) in ZnSe. The interstitial ion is surrounded by four nearest-neighbor Se ions (light-gray spheres) and six next-nearest-neighbor Zn ions (dark-gray spheres). The relaxation conserves the T_d symmetry of the ideal interstitial site. The distances of the atoms from the interstitial ion are given in percent of the bond length in the ideal lattice.

value of 1.58 eV for the doubly-positive charge state is in close agreement with the 1.61 eV obtained by Garcia and Northrup.[13] On the other hand, our value of 0.49 eV for the neutral charge state means a clearly stronger relaxation effect than their value of 0.15 eV. This difference may be caused by different relaxation modes, but Garcia and Northrup do not specify the symmetry of the relaxed vacancy. According to our calculations, the transition level between the $2+$ to 0 charge states is located at 1.35 eV above the valence-band maximum. This negative U level is about 0.3 eV lower in energy than the one obtained by Garcia and Northrup,[13] reflecting mainly the difference in the relaxation energy for the neutral charge state. The formation energies of the doubly positive Se vacancy calculated from our values given in Table I are slightly higher than those given by Garcia and Northrup.[13] This may be due to the differences in atomic chemical potentials.

The lattice relaxation around the doubly positive zinc interstitial at the tetrahedral site surrounded by selenium ions is shown in Fig. 2. The relaxation conserves the T_d symmetry of the ideal interstitial site. The nearest-neighbor Se ions relax slightly outwards, whereas the outward relaxations of the next-nearest-neighbor Zn ions are relatively larger. The formation energy for the zinc interstitial corresponding to all the possible values of the electron or atomic chemical potentials is low (see Table I). This would favor their abundance. However, according to Rong and Watkins, zinc interstitials are mobile even at quite low temperatures,[23] and thus isolated zinc interstitials are not very likely to exist in large concentrations.

The formation energies for the zinc interstitial obtained by Garcia and Northrup[13] are about 1 eV higher than ours. This is the most important difference in the formation energies between the two works. Therefore we have tested our plane-wave pseudopotential (PWPP) scheme by performing[20] all-electron calculations using the full-potential linear-muffin-tin orbital (FP-LMTO) method.[24] Since the formation energy difference between the doubly positive zinc interstitial and the doubly positive selenium vacancy does not depend on the chemical potential of the electron or the zinc or selenium atom in ZnSe, it provides an excellent test case. The results of our calculations as well as other published results are presented in Table II. Compared with the all-electron calculations our plane-wave pseudopotential calculations give quite accurate results while the results of the other groups deviate strongly from the FP-LMTO results.

TABLE II. Formation energy difference between the doubly positive zinc interstitial and the doubly positive selenium vacancy in ZnSe. All the energies given are in eV.

Method	Relaxations	$\Omega(\mathrm{Zn}_i^{2+})-\Omega(V_{\mathrm{Se}}^{2+})$
FP-LMTO[a]	No	−2.3
PWPP (64 atom)[b]	No	−2.27
PWPP (32 atom)[c]	No	−1.06
PWPP (32 atom)[d]	No	−0.60
FP-LMTO[a]	Yes[e]	−1.7
PWPP (64 atom)[b]	Yes	−1.29
PWPP (32 atom)[d]	Yes	0.31

[a]Reference 20.
[b]This work.
[c]Reference 5.
[d]Reference 13.
[e]The ionic configuration is taken from the pseudopotential calculation, total energies are calculated using the FP-LMTO method.

In n-type ZnSe the most important native defect is the zinc vacancy. This is clearly seen in Fig. 3, which gives the formation energies of the most abundant native defects in ZnSe. Actually, we have found for the zinc vacancy surely only the doubly negative charge state having the T_d symmetry. If we reduce the charge of the supercell, the hole states are very delocalized and lie near the top of the valence band indicating the lack of deep states in the band gap. The result is in contradiction with the optical detection of magnetic resonance (ODMR) experiments by Jeon, Gislason, and Watkins[25] who are able to extract the $(2-/-)$ ionization energy for the zinc vacancy and observe a Jahn-Teller relaxation in the singly negative charge state. The local density or the supercell approximation may affect the theoretical result.

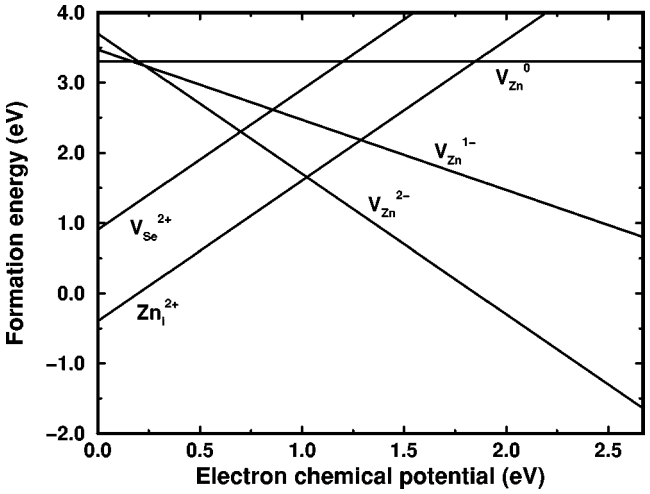

FIG. 3. Formation energies for native defects in ZnSe as a function of the electron chemical potential. Formation energies are calculated from Eq. (2.1) with $\lambda=0.5$, i.e., values correspond to a nearly stoichiometric material.

B. Nitrogen-impurity defects

The acceptor levels induced by a nitrogen ion in ZnSe are relatively low in energy, because there are no p electrons in the ion core. As a consequence, we find that the substitutional nitrogen at the Se site (N_{Se}) is in the negative charge state for all the positions of the Fermi level in the band gap. This means that the negative ion can in reality bind a hole into an effective-mass state just above the top of the valence band. The ionization of the bound hole will then lead to a delocalized hole at the top of the valence band. This is in accord with the calculations by Kwak, King-Smith, and Vanderbilt[26] for the hole density corresponding to the neutral N_{Se} showing that the hole density is very delocalized in the supercell used. Moreover, according to the experiments for the substitutional nitrogen in ZnSe only one ionization energy of about 0.11 eV above the top of the valence band has been found.[27]

The nitrogen ion has a relatively small ionic radius and therefore the lattice relaxation around the substitutional N_{Se} is quite large. The neighboring Zn ions relax symmetrically *inwards* from the ideal sites by $\sim 18\%$ of the bulk bond length. We believe that the large lattice relaxation is an important reason for the partial success of nitrogen as a dopant in ZnSe. The energy lowering associated with the relaxation is 3.9 eV. This relaxation energy lowers the formation energy of N_{Se} and increases the stability of the defect. In comparison, the relaxation energy for the substitutional As impurity in ZnSe $(As_{Se})^{1-}$ is only 0.14 eV.[13]

The nitrogen interstitials [$N_i(T_{Zn})$ and $N_i(T_{Se})$] and the ''antisite'' defect (N_{Zn}) have high formation energies for all values of μ_e within the band gap and for all allowed values of μ_{Zn} as compared with the substitutional $N_{Se}{}^{1-}$.[20] Therefore the simplest nitrogen-related point defects are unlikely to cause acceptor compensation.

C. Nitrogen-impurity–native-defect complexes

Garcia and Northrup have suggested that formation of defect complexes containing the acceptor impurity may cause the compensation responsible for the saturation of the hole concentration in ZnSe.[13] The most obvious candidates for compensating defect complexes are the pairs formed between the substitutional nitrogen impurity and the Zn interstitial ($N_{Se}Zn_i$) or the Se vacancy ($N_{Se}V_{Se}$). Also the nitrogen dimers (N_2) have been suggested to form compensating defect complexes in ZnSe.[12] However, the formation of the nitrogen dimers during the growth process is improbable because atomic nitrogen sources are used and the total nitrogen concentration is orders of magnitude lower than that of host Zn and Se atoms. Therefore we do not consider the nitrogen dimer in this work. As a matter of fact, a reliable comparison of the formation energies of defects containing different numbers of nitrogen atoms is also difficult because of the uncertainty in the value of the nitrogen chemical potential (μ_N). A split-interstitial $(N\text{-}N)_{Se}$ complex could act as a compensating center, since the most stable charge state for it is $2+$.[12,20] Thus, the presence of compensating split interstitials could also be the reason for the failure of N doping using molecular nitrogen. The formation energies for various defect complexes containing one nitrogen impurity are collected in Table III.

TABLE III. Nitrogen-impurity-defect complexes in ZnSe with the lowest formation energies. The formation energies [Eq. (2.1)], binding energies (E_B), and ionization levels for the complexes are shown. All the energies given are in eV.

Defect	Formation energy	E_B	Ionization levels
$(N_{Se})^-$	$0.01+\lambda\Delta H-\mu_e$		
$(N_{Se}V_{Se})^{1+}$	$-0.72+2\lambda\Delta H+\mu_e$	0.87	$(+/0)$ 2.00
$(N_{Se}V_{Se})^0$	$1.29+2\lambda\Delta H$		$(0/-)$ 1.05
$(N_{Se}V_{Se})^{1-}$	$2.34+2\lambda\Delta H-\mu_e$	0.22	$(+/-)$ 1.53
$(N_{Se}Zn_i)^{1+}$	$-2.43+2\lambda\Delta H+\mu_e$	1.28	
$(N_{Se}V_{Se}Zn_i)^{1+}$	$-0.78+3\lambda\Delta H+\mu_e$	1.97	

The next-nearest-neighbor $N_{Se}V_{Se}$ pair has three possible charge states, $1+$, 0, and $1-$, from which the neutral one is metastable. The negative-U transition $(+/-)$ is 1.53 eV above the valence-band maximum. This level corresponds to the $(2+/0)$ level of the selenium vacancy; the Coulomb repulsion due to the negative nitrogen end of the defect has pushed the level upwards in energy. The ionic relaxation around the $N_{Se}V_{Se}$ pair resembles those of isolated N_{Se} and V_{Se} (see Fig. 4). The Zn ions around N_{Se} relax inwards about $\sim 18\%$ in both charge states. In the positive charge state the nearest neighbors of the selenium vacancy end of $N_{Se}V_{Se}$ relax outwards ~ 25 percent. This strong outwards relaxation changes to strong ($\sim 22\%$) inwards relaxation as the charge state of the defect changes from positive to negative, except for that zinc ion, which is the nearest neighbor for both ends (N_{Se} and V_{Se}) of the defect pair. Thus, in both charge states the defect pair can benefit from the release of elastic strain energy with respect to two isolated defects. A large relax-

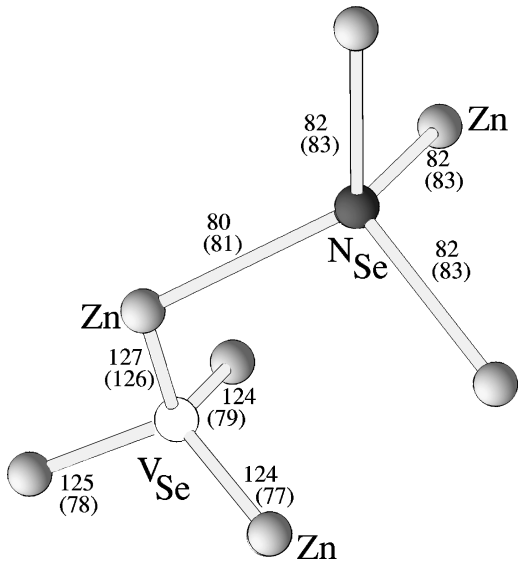

FIG. 4. Ionic structure of the $N_{Se}V_{Se}$ defect pair. The center of the vacancy (white sphere) is defined as the position of a Se atom in a perfect lattice and by thinking that atoms far from the defects of the defect superlattice do not remarkably move from their ideal lattice positions. The distances of the Zn ions (light-gray spheres) from the vacancy center and from the N ion (dark-gray sphere) are given in percent of the bond length in the ideal lattice for the positive (upper numbers) and for the negative (numbers in parentheses) charge states.

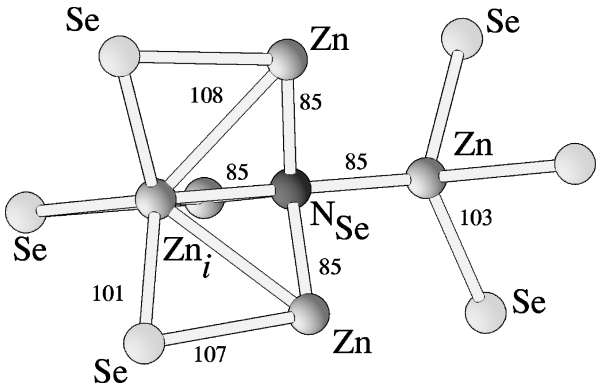

FIG. 5. Ionic structure of the $N_{Se}Zn_i$ defect pair. The distances between the atoms are given in percent of the bond length in the ideal lattice.

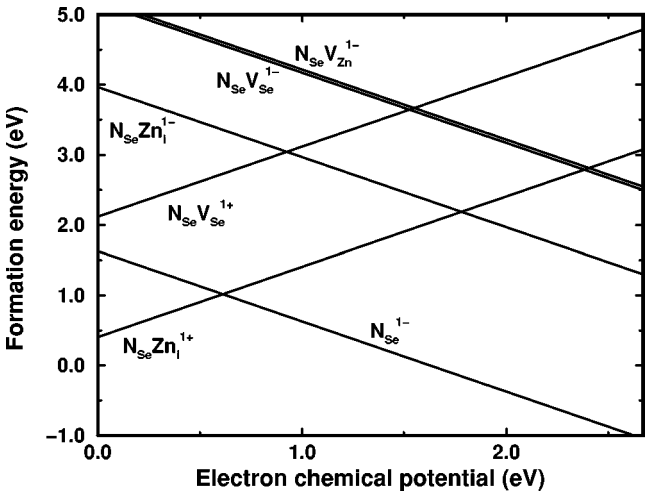

FIG. 6. Nitrogen-related defects in ZnSe with the lowest formation energies. The formation energies are shown as a function of electron chemical potential for ZnSe grown under Se-rich conditions ($\lambda = 0.8$).

ation energy of ~ 5 eV results from the large ionic relaxation around $N_{Se}V_{Se}$ pair in both stable charge states.

There is experimental evidence for the existence of the $N_{Se}V_{Se}$ pairs in ZnSe. Hauksson *et al.*[28] suggested the presence for the $N_{Se}V_{Se}$ pair in heavily N-doped ZnSe. Recently, Saarinen *et al.*[29] have observed, using positron annihilation experiments, Se vacancies in N-doped ZnSe samples. They showed that the concentration of Se vacancies in N-doped samples is comparable to the concentration of nitrogen in the samples measured. Since only neutral and negative vacancies trap positrons and the isolated selenium vacancy in *p*-type ZnSe is expected to be in a doubly positive charge state,[20,13] Saarinen *et al.* concluded that the observed Se vacancy has to be a part of a defect complex and suggested it to be $N_{Se}V_{Se}$. The existence of both the negative and positive charge states for $N_{Se}V_{Se}$ opens an interesting possibility that this defect may first act like an acceptor, but when the Fermi level is lowered due to increasing doping the defect begins to act as a compensating center.

The release of the elastic energy in the formation of the $(N_{Se}V_{Se})^{1+}$ pair results in a binding energy of 0.87 eV between $N_{Se}{}^{-}$ and $V_{Se}{}^{2+}$. This lowers the formation energy of the defect pair. The nearest-neighbor $(N_{Se}Zn_i)^{1+}$ is even more tightly bound, the binding energy is 1.28 eV. Since the formation energy for the Zn interstitial is about 1.3 eV lower than that for the Se vacancy, the nearest-neighbor $(N_{Se}Zn_i)^{1+}$ is the lowest formation energy defect in ZnSe. The difference in the formation energy between these two compensating (i.e., positive) defect pairs is 1.7 eV regardless of the stoichiometry and the electron chemical potential. In the $N_{Se}Zn_i$ pair the substitutional nitrogen ion introduces a strong inward relaxation of the surrounding five Zn ions (one interstitial and four in the neighboring lattice sites). This strong lattice relaxation decreases also the distances between the interstitial zinc atom and its next-nearest-neighbor zinc atoms so that the interstitial zinc atoms has effectively seven nearest neighbors (one nitrogen, three selenium, and three zinc atoms; see Fig. 5). The increase of the coordination number of the ions in the defect pair seems to be the reason for the binding of $N_{Se}Zn_i$ rather than the release of the elastic energy. Before drawing firm conclusions one should bear in mind that the crystal growth process is not a thermodynamic equilibrium process. Therefore one should be cautious in using the formation energies to estimate the concentrations (or the concentration differences) of the defects. For example, it is possible that the concentration of the $N_{Se}Zn_i$ pair is not very high even though the calculated formation energy is low.

The increase in the parameter λ in Eq. (2.1) dictating the stoichiometry favors the generation of the substitutional nitrogen acceptor over the compensating centers (see Table III). Therefore the best growth conditions to obtain the highest effective acceptor concentrations are selenium-rich conditions. Figure 6 shows as a function of the electron chemical potential the formation energies for those nitrogen-related defects that have the lowest formation energies in ZnSe grown under Se-rich conditions ($\lambda = 0.8$). As the Fermi level goes down, for example, due to the nitrogen doping, the formation energy of the acceptor impurity rises, and the formation of defect complexes containing nitrogen becomes more favored. Thus, these defect complexes may incorporate the further nitrogen dissolved in ZnSe and result in a decrease of the doping efficiency.

Our results indicate that the success of nitrogen as a dopant in ZnSe is connected to the large lattice relaxation. The relaxation energy for the isolated substitutional N impurity is 3.9 eV, which is 0.2 eV more than that for the most probable compensation center, the $(N_{Se}Zn_i)^{1+}$ pair. If the N impurity is replaced by another group-V element (such as As) the relaxation energy of the compensating impurity-interstitial pair is larger than that of the isolated acceptor impurity. In the case of As doping, the difference is about 0.4 eV. Therefore the formation of the negative acceptor impurity instead of the impurity-interstitial pair is more favored in the case of N doping than in the case of As doping. Energetically this difference between the N and As doping is 0.6 eV which at the temperature of 500 K means a factor of $\exp(0.6\ \text{eV}/k_BT) = 10^6$ in the concentration.

In order to demonstrate that point-defect clusters are easily formed in ZnSe we have calculated also the complex $N_{Se}V_{Se}Zn_i$ (see Fig. 7 for the structure). It could be a consequence of the following reaction: a negative $N_{Se}V_{Se}$ defect produced during the growth process traps a doubly positive mobile zinc interstitial. The binding energy associated with

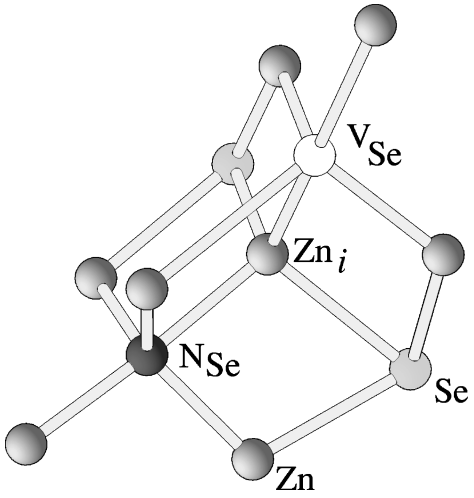

FIG. 7. Ionic structure of the $N_{Se}V_{Se}Zn_i$ defect. The lattice relaxation around this defect follows closely the ones obtained for the isolated constituents, i.e., the nearest neighbors of the substitutional nitrogen relax inwards about 15–20 %, the lattice relaxation is small around the zinc interstitial, and a strongly charge-state-dependent relaxation is observed around the selenium vacancy.

the positive $N_{Se}V_{Se}Zn_i$ defect formed by the negative $N_{Se}V_{Se}$ and the doubly positive Zn_i is rather large, ~ 1.97 eV. This tendency of the defects to bind strongly into small defect clusters can eventually be one of the reasons for the degradation of the ZnSe-based devices.

IV. CONCLUSIONS

Our calculations reveal that defect complexes formed by a substitutional nitrogen dopant with a zinc interstitial or a selenium vacancy in ZnSe have low formation energies and relatively large binding energies. These properties favor their creation. These defect complexes are positively charged in *p*-type materials and therefore they can act as compensating defects and cause the saturation of the hole concentration in N doping.

The success of N doping in comparison with, for example, As doping is connected with the lattice relaxation around the dopant atom. For the N doping the lattice relaxation lowers the formation energy of the substitutional impurity with respect to the compensating defect having the lowest formation energy. In the case of As doping the opposite occurs. Selenium-rich growth conditions should lead to the highest active acceptor concentrations in nitrogen doping of ZnSe.

Our results also show that the formation of larger point-defect clusters in ZnSe is energetically favored. This will lead to the aggregation of dopant atoms and point defects into clusters, which may trigger the mechanical degradation of the material and thus contribute to the short lifetime of ZnSe-based optoelectronic devices.

ACKNOWLEDGMENTS

The authors wish to thank Professor P. Hautojärvi, Dr. K. Saarinen, Professor K. Laasonen, and Dr. T. Mattila for many valuable discussions. This work has been supported by the Academy of Finland through a MATRA grant. We also acknowledge the generous computing resources of the Center for the Scientific Computing (CSC), Espoo, Finland. One of us (S.P.) wishes to thank Dr. Stewart Clark, the EU TRACS program, and Edinburgh Parallel Computing Center (EPCC) for the help in parallel computing.

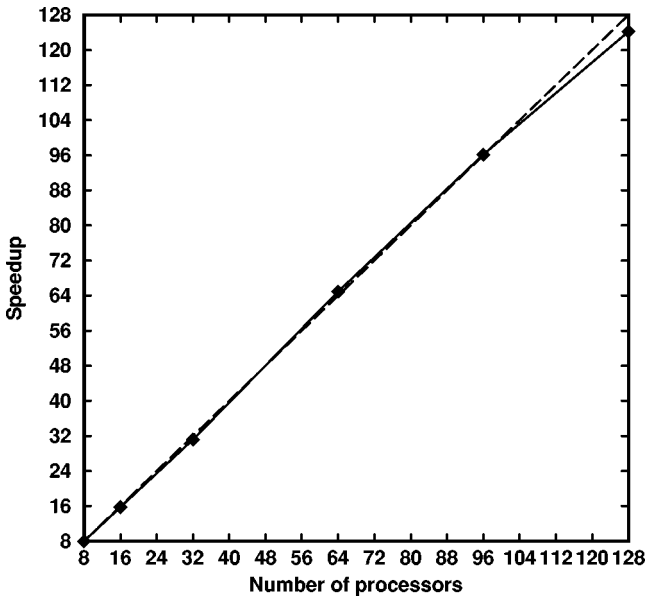

FIG. 8. Speedup vs the number of processors for the FINGER code running in a CRAY-T3E system. The dashed line corresponds to the ideal speedup. Employing 128 processors we reach about 10 Gflops sustained speed. The system used in this scaling test has been the zinc vacancy described by the 64-atomic-site supercell and four **k** points.

APPENDIX: PARALLEL PWPP CODE (FINGER)

The computational task of a plane-wave pseudopotential code employing the DFT within Kohn-Sham formalism is to find the set of plane-wave coefficients $c(n_{\rm pw},n_{\rm states},n_{\rm kpts})$ generating the one-electron wave functions

$$\Psi_j(\mathbf{r})=\sum_{\mathbf{k}} w_{\mathbf{k}} \sum_{\mathbf{G}} c(\mathbf{G},j,\mathbf{k}) \exp\left[i(\mathbf{k}+\mathbf{G})\cdot\mathbf{r}\right], \quad \text{(A1)}$$

which minimizes the total-energy functional,

$$E[\{\Psi_i\},\{R_I\}]=\sum_i f_i \int d\mathbf{r}\Psi_i^*[-\tfrac{1}{2}\nabla^2]\Psi_i + \tfrac{1}{2}\int d\mathbf{r}d\mathbf{r}'\frac{n(\mathbf{r})n(\mathbf{r}')}{|\mathbf{r}-\mathbf{r}'|}+\int d\mathbf{r}V_{\rm ion}(\mathbf{r})n(\mathbf{r}) + E_{\rm ion}(\{\mathbf{R}_I\})+E_{\rm xc}[n(\mathbf{r})]. \quad \text{(A2)}$$

Above, the electron density $n(\mathbf{r})$ is given by

$$n(\mathbf{r})=\sum_i f_i|\Psi(\mathbf{r})|^2. \quad \text{(A3)}$$

The plane-wave expansion of the wave functions (A1) provides three data-driven ways to divide the computation: one can divide by (i) **k** points, (ii) states, and (iii) **G** vectors.[30] Of these three strategies the first two are useful in

small parallel machines, but in the massively parallel machines only strategy (iii) is effective. The details of each parallelization strategy can be found from Refs. 30, and 31. Each of these parallelization strategies requires substantial communication with every processor participating in the calculation.

Linking together two or three of the above-mentioned parallelization strategies leads to a situation where all of the calculations are done within small blocks of processors and all interprocessor communication is done within these small blocks instead of communicating over all participating processors. In the FINGER code approaches (i) and (ii) are used simultaneously. We have first divided processors into n_{kpts} blocks of processors so that in each block the processors correspond to the same **k** point. Real and reciprocal spaces are divided inside of these blocks. Calculations in these n_{kpts} blocks are relatively independent of each other and, in principle, only the total electron density has to be globally summed over these blocks. Inside each of the n_{kpts} block the **G**-vector parallelization is used. The most difficult part in the **G**-vector parallelization is the parallelization of the fast Fourier transforms (FFT's). We have followed in the FINGER code the very effective FFT parallelization introduced originally in CETEP (Cambridge Edinburgh Total Energy Package) code.[30,32] The speedup for the FINGER code as the number of processors is increased is shown in Fig. 8. The ideal speedup shown in Fig. 8 does not really tell anything about the performance of a code in a parallel machine without the knowledge of the speed/processor the code obtains. Using the FINGER code we get up to 130 Mflops/processor sustained speed in a CRAY-T3E computer system.[33]

*Electronic address: Sami.Poykko@hut.fi
†Electronic address: Martti.Puska@hut.fi
‡Electronic address: Risto.Nieminen@hut.fi

[1] Pauline Rigby, Nature (London) **384**, 610 (1996).
[2] R. M. Park, M. B. Troffer, J. M. DePuydt, and M. A. Haase, Appl. Phys. Lett. **57**, 2127 (1990).
[3] K. Ohkawa, T. Karasawa, and T. J. Mitsuyo, J. Cryst. Growth **111**, 797 (1991).
[4] D. B. Laks, C. G. Van de Walle, G. F. Neumark, and S. T. Pantelides, Phys. Rev. Lett. **66**, 648 (1991).
[5] D. B. Laks, C. G. Van de Walle, G. F. Neumark, P. E. Blöchl, and S. T. Pantelides, Phys. Rev. B **45**, 10 965 (1992).
[6] Z. Zhu, G. Horsburgh, P. J. Thompson, G. D. Brownlie, S. Y. Wang, K. A. Prior, and B. C. Cavenett, Appl. Phys. Lett. **67**, 3927 (1995).
[7] D. J. Chadi and K. J. Chang, Appl. Phys. Lett. **55**, 575 (1989).
[8] D. J. Chadi, Appl. Phys. Lett. **59**, 3589 (1991).
[9] D. J. Chadi and N. J. Troullier, Physica B **185**, 128 (1993).
[10] D. J. Chadi, Phys. Rev. Lett. **72**, 534 (1994).
[11] C. H. Park and D. J. Chadi, Phys. Rev. Lett. **75**, 1134 (1995).
[12] Byoung-Ho Cheong, C. H. Park, and K. J. Chang, Phys. Rev. B **51**, 10 610 (1995).
[13] A. Garcia and J. E. Northrup, Phys. Rev. Lett. **74**, 1131 (1995).
[14] D. M. Ceperley and B. J. Alder, Phys. Rev. Lett. **45**, 566 (1980); J. P. Perdew and A. Zunger, Phys. Rev. B **23**, 5048 (1981).
[15] D. J. Chadi and M. L. Cohen, Phys. Rev. B **8**, 5747 (1973).
[16] S. Pöykkö, M. J. Puska, M. Alatalo, and R. M. Nieminen, Phys. Rev. B **54**, 7909 (1996).
[17] D. R. Hamann, Phys. Rev. B **40**, 2980 (1989).
[18] S. G. Louie, S. Froyen, and M. L. Cohen, Phys. Rev. B **26**, 1738 (1982).
[19] D. Vanderbilt, Phys. Rev. B **41**, 7892 (1990); K. Laasonen, A. Pasquarello, R. Car, C. Lee, and D. Vanderbilt, *ibid.* **47**, 10 142 (1993).
[20] S. Pöykkö, M. J. Puska, T. Korhonen, and R. M. Nieminen, Mater. Sci. Eng. B **43**, 1 (1997).
[21] The cohesive energy of a nitrogen dimer (as compared with a calculation employing the 50 Ry plane-wave cutoff) is converged within 20 meV, and the equilibrium distance within 2.0×10^{-4} Å.
[22] See, for example, W. H. Press, S. A. Teukolsky, W. T. Vetterling, and B. P. Flannery, *Numerical Recipes* (Cambridge University Press, Cambridge, England, 1992).
[23] F. Rong and G. D. Watkins, Phys. Rev. Lett. **58**, 1486 (1987).
[24] M. Methfessel, Phys. Rev. B **38**, 1537 (1988); M. Methfessel, C. O. Rodriguez, and O. K. Andersen, *ibid.* **40**, 2009 (1989).
[25] Duk Y. Jeon, H. P. Gislason, and G. D. Watkins, Phys. Rev. B **48**, 7872 (1993).
[26] K. W. Kwak, R. D. King-Smith, and D. Vanderbilt, Phys. Rev. B **48**, 17 827 (1993).
[27] K. Kosai *et al.*, Appl. Phys. Lett. **35**, 194 (1979).
[28] I. S. Hauksson, J. Simpson, S. Y. Wang, K. A. Prior, and B. C. Cavenett, Appl. Phys. Lett. **61**, 2208 (1992).
[29] K. Saarinen, T. Laine, K. Skog, J. Mäkinen, P. Hautojärvi, K. Rakennus, P. Uusimaa, A. Salokatve, and M. Pessa, Phys. Rev. Lett. **77**, 3407 (1996).
[30] L. J. Clarke, I. Štich, and M. C. Payne, Comput. Phys. Commun. **72**, 14 (1992).
[31] J. S. Nelson, S. J. Plimpton, and M. P. Sears, Phys. Rev. B **47**, 1765 (1993).
[32] M. C. Payne, M. P. Teter, D. C. Allan, T. A. Arias, and J. D. Joannopoulos, Rev. Mod. Phys. **64**, 1045 (1992).
[33] Our estimate for the Mflops/processor rate is obtained using the *pat* performance analysis tool in Cray-T3E (375 MHz DEC alpha processors).